Available online at www.sciencedirect.com
ScienceDirect
Physics Letters B 659 (2008) 80–86
PHYSICS LETTERS B
www.elsevier.com/locate/physletb

Study of the decay mechanism for $B^+ \to p\bar{p}K^+$ and $B^+ \to p\bar{p}\pi^+$

Belle Collaboration

J.-T. Wei [z], M.-Z. Wang [z], I. Adachi [g], H. Aihara [aq], V. Aulchenko [a], T. Aushev [r,m], A.M. Bakich [am], V. Balagura [m], E. Barberio [u], A. Bay [r], K. Belous [k], U. Bitenc [n], A. Bondar [a], A. Bozek [aa], M. Bračko [t,n], T.E. Browder [f], P. Chang [z], Y. Chao [z], A. Chen [x], K.-F. Chen [z], B.G. Cheon [e], C.-C. Chiang [z], I.-S. Cho [au], Y. Choi [al], Y.K. Choi [al], S. Cole [am], M. Danilov [m], M. Dash [at], A. Drutskoy [c], S. Eidelman [a], S. Fratina [n], N. Gabyshev [a], B. Golob [s,n], H. Ha [p], J. Haba [g], T. Hara [af], K. Hayasaka [v], H. Hayashii [w], M. Hazumi [g], D. Heffernan [af], T. Hokuue [v], Y. Hoshi [ao], Y.B. Hsiung [z], H.J. Hyun [q], T. Iijima [v], K. Ikado [v], K. Inami [v], A. Ishikawa [aq], R. Itoh [g], M. Iwasaki [aq], Y. Iwasaki [g], D.H. Kah [q], J.H. Kang [au], N. Katayama [g], H. Kawai [b], T. Kawasaki [ac], H. Kichimi [g], Y.J. Kim [d], K. Kinoshita [c], S. Korpar [t,n], P. Križan [s,n], P. Krokovny [g], R. Kumar [ag], C.C. Kuo [x], A. Kuzmin [a], Y.-J. Kwon [au], J.S. Lee [al], S.E. Lee [ak], T. Lesiak [aa], S.-W. Lin [z], Y. Liu [d], D. Liventsev [m], F. Mandl [l], T. Matsumoto [ar], A. Matyja [aa], S. McOnie [am], T. Medvedeva [m], W. Mitaroff [l], K. Miyabayashi [w], H. Miyake [af], H. Miyata [ac], Y. Miyazaki [v], R. Mizuk [m], Y. Nagasaka [h], E. Nakano [ae], M. Nakao [g], S. Nishida [g], O. Nitoh [as], S. Ogawa [an], T. Ohshima [v], S. Okuno [o], S.L. Olsen [f], H. Ozaki [g], P. Pakhlov [m], G. Pakhlova [m], C.W. Park [al], H. Park [q], K.S. Park [al], R. Pestotnik [n], L.E. Piilonen [at], H. Sahoo [f], Y. Sakai [g], O. Schneider [r], J. Schümann [g], R. Seidl [i,ai], K. Senyo [v], M.E. Sevior [u], M. Shapkin [k], H. Shibuya [an], J.-G. Shiu [z], J.B. Singh [ag], A. Sokolov [k], A. Somov [c], S. Stanič [ad], M. Starič [n], T. Sumiyoshi [ar], O. Tajima [g], F. Takasaki [g], K. Tamai [g], M. Tanaka [g], G.N. Taylor [u], Y. Teramoto [ae], X.C. Tian [ah], I. Tikhomirov [m], T. Tsuboyama [g], S. Uehara [g], K. Ueno [z], T. Uglov [m], Y. Unno [e], S. Uno [g], P. Urquijo [u], G. Varner [f], K.E. Varvell [am], K. Vervink [r], S. Villa [r], A. Vinokurova [a], C.C. Wang [z], C.H. Wang [y], P. Wang [j], Y. Watanabe [o], R. Wedd [u], E. Won [p], A. Yamaguchi [ap], Y. Yamashita [ab], M. Yamauchi [g], C.C. Zhang [j], Z.P. Zhang [aj], V. Zhilich [a], A. Zupanc [n]

[a] *Budker Institute of Nuclear Physics, Novosibirsk, Russia*
[b] *Chiba University, Chiba, Japan*
[c] *University of Cincinnati, Cincinnati, OH, USA*
[d] *The Graduate University for Advanced Studies, Hayama, Japan*
[e] *Hanyang University, Seoul, South Korea*
[f] *University of Hawaii, Honolulu, HI, USA*
[g] *High Energy Accelerator Research Organization (KEK), Tsukuba, Japan*
[h] *Hiroshima Institute of Technology, Hiroshima, Japan*
[i] *University of Illinois at Urbana-Champaign, Urbana, IL, USA*
[j] *Institute of High Energy Physics, Chinese Academy of Sciences, Beijing, PR China*
[k] *Institute for High Energy Physics, Protvino, Russia*
[l] *Institute of High Energy Physics, Vienna, Austria*
[m] *Institute for Theoretical and Experimental Physics, Moscow, Russia*
[n] *J. Stefan Institute, Ljubljana, Slovenia*
[o] *Kanagawa University, Yokohama, Japan*
[p] *Korea University, Seoul, South Korea*
[q] *Kyungpook National University, Taegu, South Korea*
[r] *Swiss Federal Institute of Technology of Lausanne, EPFL, Lausanne, Switzerland*
[s] *University of Ljubljana, Ljubljana, Slovenia*

0370-2693/$ – see front matter
doi:10.1016/j.physletb.2007.11.063

[t] University of Maribor, Maribor, Slovenia
[u] University of Melbourne, Victoria, Australia
[v] Nagoya University, Nagoya, Japan
[w] Nara Women's University, Nara, Japan
[x] National Central University, Chung-li, Taiwan
[y] National United University, Miao Li, Taiwan
[z] Department of Physics, National Taiwan University, Taipei, Taiwan
[aa] H. Niewodniczanski Institute of Nuclear Physics, Krakow, Poland
[ab] Nippon Dental University, Niigata, Japan
[ac] Niigata University, Niigata, Japan
[ad] University of Nova Gorica, Nova Gorica, Slovenia
[ae] Osaka City University, Osaka, Japan
[af] Osaka University, Osaka, Japan
[ag] Panjab University, Chandigarh, India
[ah] Peking University, Beijing, PR China
[ai] RIKEN BNL Research Center, Brookhaven, NY, USA
[aj] University of Science and Technology of China, Hefei, PR China
[ak] Seoul National University, Seoul, South Korea
[al] Sungkyunkwan University, Suwon, South Korea
[am] University of Sydney, Sydney, NSW, Australia
[an] Toho University, Funabashi, Japan
[ao] Tohoku Gakuin University, Tagajo, Japan
[ap] Tohoku University, Sendai, Japan
[aq] Department of Physics, University of Tokyo, Tokyo, Japan
[ar] Tokyo Metropolitan University, Tokyo, Japan
[as] Tokyo University of Agriculture and Technology, Tokyo, Japan
[at] Virginia Polytechnic Institute and State University, Blacksburg, VA, USA
[au] Yonsei University, Seoul, South Korea

Received 28 June 2007; received in revised form 14 September 2007; accepted 17 November 2007

Available online 3 December 2007

Editor: M. Doser

Abstract

We study the characteristics of the low mass $p\bar{p}$ enhancements near threshold in the three-body decays $B^+ \to p\bar{p}K^+$ and $B^+ \to p\bar{p}\pi^+$. We observe that the proton polar angle distributions in the $p\bar{p}$ helicity frame in the two decays have the opposite polarity, and measure the forward-backward asymmetries as a function of the $p\bar{p}$ mass for the $p\bar{p}K^+$ mode. We also search for the intermediate two-body decays, $B^+ \to \bar{p}\Delta^{++}$ and $B^+ \to p\bar{\Delta}^0$, and set upper limits on their branching fractions. These results are obtained from a 414 fb^{-1} data sample that contains $449 \times 10^6 B\bar{B}$ events collected near the $\Upsilon(4S)$ resonance with the Belle detector at the KEKB asymmetric-energy e^+e^- collider.

PACS: 13.25.Hw

After the first observation of the charmless baryonic B meson decay, $B^+ \to p\bar{p}K^+$ [1],[1] many three-body baryonic decays were found [2–5]. The dominant contributions for these decays are presumably via the $b \to s$ penguin diagram, shown in Fig. 1(a); however $B^+ \to p\bar{p}\pi^+$ is believed to proceed via the $b \to u$ tree diagram as shown in Fig. 1(b). One interesting feature of these decays is that the dibaryon mass spectra show enhancements near threshold as conjectured in Ref. [6]. Many theoretical explanations [7] have been proposed to describe these enhancements in the dibaryon system, which seem to be a universal feature of all charmless baryonic B decays. Study of the proton polar angular distribution for the dibaryon system in the $p\bar{p}K^+$ mode [8] indicates a violation of the $b \to s$ short distance picture [9]. Explicit predictions for the dibaryon mass spectra [10] and the angular distributions [11,12] for $B^+ \to p\bar{p}K^+/\pi^+$ became available after the experimental findings were reported.

In this Letter, we study the three-body charmless baryonic B meson decays $B^+ \to p\bar{p}K^+$ and $B^+ \to p\bar{p}\pi^+$. The differential branching fractions as a function of the dibaryon mass and the polar angle distributions of the proton in the dibaryon system are presented. We also search for intermediate two-body decays in $p\bar{p}\pi^+$ three-body final states. This is motivated by the observations of two-body decays of charmed baryons [13]. Many predictions based on QCD sum rules [14], pole models [15] and a topological approach [16] indicate that $B^+ \to \bar{p}\Delta^{++}$ and $B^+ \to p\bar{\Delta}^0$ should be observable in the large data samples accumulated at the B-factories.

We use a 414 fb^{-1} data sample, corresponding to $449 \times 10^6 B\bar{B}$ pairs, collected with the Belle detector at the KEKB

[1] Throughout this Letter, inclusion of charge conjugate mode is always implied unless otherwise stated.

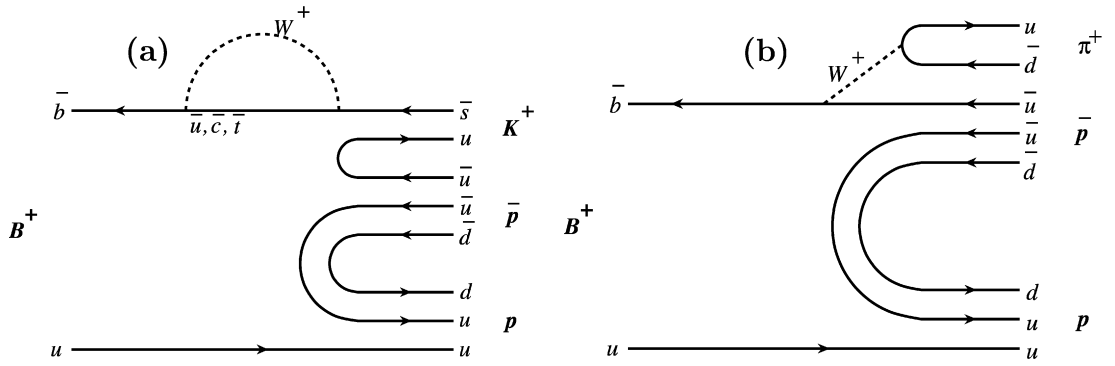

Fig. 1. The possible leading (a) $b \to s$ penguin diagram and (b) $b \to u$ tree diagram for $B^+ \to p\bar{p}K^+$ and $B^+ \to p\bar{p}\pi^+$ decays, respectively.

asymmetric-energy e^+e^- (3.5 on 8 GeV) collider [17]. The Belle detector is a large-solid-angle magnetic spectrometer that consists of a silicon vertex detector (SVD), a 50-layer central drift chamber (CDC), an array of aerogel threshold Cherenkov counters (ACC), a barrel-like arrangement of time-of-flight scintillation counters (TOF), and an electromagnetic calorimeter composed of CsI(Tl) crystals located inside a superconducting solenoid coil that provides a 1.5 T magnetic field. An iron flux-return located outside of the coil is instrumented to detect K_L^0 mesons and to identify muons. The detector is described in detail elsewhere [18]. Two inner detector configurations were used. A 2.0 cm beampipe and a 3-layer silicon vertex detector were used for the first sample of $152 \times 10^6 B\bar{B}$ pairs, while a 1.5 cm beampipe, a 4-layer silicon detector and a small-cell inner drift chamber were used to record the remaining $297 \times 10^6 B\bar{B}$ pairs [19].

The event selection criteria are based on information obtained from the tracking system (SVD and CDC) and the hadron identification system (CDC, ACC, and TOF). All primary charged tracks are required to satisfy track quality criteria based on the track impact parameters relative to the interaction point (IP). The deviations from the IP position are required to be within ± 0.3 cm in the transverse (x–y) plane, and within ± 3 cm in the z direction, where the z axis is opposite the positron beam direction. For each track, the likelihood values L_p, L_K, and L_π that it is a proton, kaon, or pion, respectively, are determined from the information provided by the hadron identification system. The track is identified as a proton if $L_p/(L_p + L_K) > 0.6$ and $L_p/(L_p + L_\pi) > 0.6$, or as a kaon if $L_K/(L_K + L_\pi) > 0.6$, or as a pion if $L_\pi/(L_K + L_\pi) > 0.6$. For particles with momenta at 2 GeV/c, the proton selection efficiency is about 84% (88% for p and 80% for $\bar{p}$) and the fake rate is about 10% for kaons and 3% for pions; the kaon selection efficiency is about 85% and the pion to kaon fake rate is about 2%; the pion selection efficiency is about 88% and the kaon to pion fake rate is about 11%.

Candidate B mesons are reconstructed in the $B^+ \to p\bar{p}K^+$ and $B^+ \to p\bar{p}\pi^+$ modes. We use two kinematic variables in the center of mass (CM) frame to identify the reconstructed B meson candidates: the beam energy constrained mass $M_{\rm bc} = \sqrt{E_{\rm beam}^2 - p_B^2}$, and the energy difference $\Delta E = E_B - E_{\rm beam}$, where $E_{\rm beam}$ is the beam energy, and p_B and E_B are the momentum and energy, respectively, of the reconstructed B meson. The candidate region is defined as $5.20\ {\rm GeV}/c^2 < M_{\rm bc} < 5.29\ {\rm GeV}/c^2$ and $-0.1\ {\rm GeV} < \Delta E < 0.3\ {\rm GeV}$. The lower bound in ΔE for candidate events is chosen to exclude possible cross-feed background from the decays with additional pions to the search modes, e.g. $B^+ \to p\bar{p}K^{*+}$. From a GEANT [20] based Monte Carlo (MC) simulation, the signal peaks in a signal box defined by $5.27\ {\rm GeV}/c^2 < M_{\rm bc} < 5.29\ {\rm GeV}/c^2$ and $|\Delta E| < 0.05$ GeV, and there is no peaking background except cross-feed events between the $p\bar{p}K^+$ and $p\bar{p}\pi^+$ modes.

The background in the fit region arises dominantly from the continuum $e^+e^- \to q\bar{q}$ ($q = u, d, s, c$) process. We suppress the jet-like continuum background events relative to the more spherical $B\bar{B}$ signal events using a Fisher discriminant [21] that combines seven event shape variables, as described in Ref. [22]. Probability density functions (PDFs) for the Fisher discriminant and the cosine of the angle between the B flight direction and the beam direction in the $\Upsilon(4S)$ rest frame are combined to form the signal (background) likelihood $\mathcal{L}_s$ ($\mathcal{L}_b$). The signal PDFs are determined using signal MC simulation; the background PDFs are obtained from the sideband data with $M_{\rm bc} < 5.26\ {\rm GeV}/c^2$. We require the likelihood ratio $\mathcal{R} = \mathcal{L}_s/(\mathcal{L}_s + \mathcal{L}_b)$ to be greater than 0.75 and 0.85 for the $p\bar{p}K^+$ and $p\bar{p}\pi^+$ modes, respectively. These selection criteria are determined by optimization of $n_s/\sqrt{n_s + n_b}$, where n_s and n_b denote the expected numbers of signal and background events in the signal box, respectively. We use the branching fractions from our previous measurements [3,8] in the calculation of n_s and use the number of sideband events to estimate n_b. If there are multiple B candidates in a single event, we select the one with the best χ^2 value from the vertex fit. The fractions of multiple B events are about 8% and 10% for the $p\bar{p}K^+$ and $p\bar{p}\pi^+$ modes, respectively.

We perform an unbinned extended likelihood fit that maximizes the likelihood function,

$$L = \frac{e^{-(N_s+N_b)}}{N!} \prod_{i=1}^{N} \left[N_s P_s(M_{{\rm bc}_i}, \Delta E_i) + N_b P_b(M_{{\rm bc}_i}, \Delta E_i) \right],$$

to estimate the signal yield in the candidate region; here P_s (P_b) denotes the signal (background) PDF, N is the number of events in the fit, and N_s and N_b are fit parameters representing the number of signal and background events, respectively.

For the signal PDF, we use a Gaussian function to represent the signal $M_{\rm bc}$ and a double Gaussian for ΔE with parameters

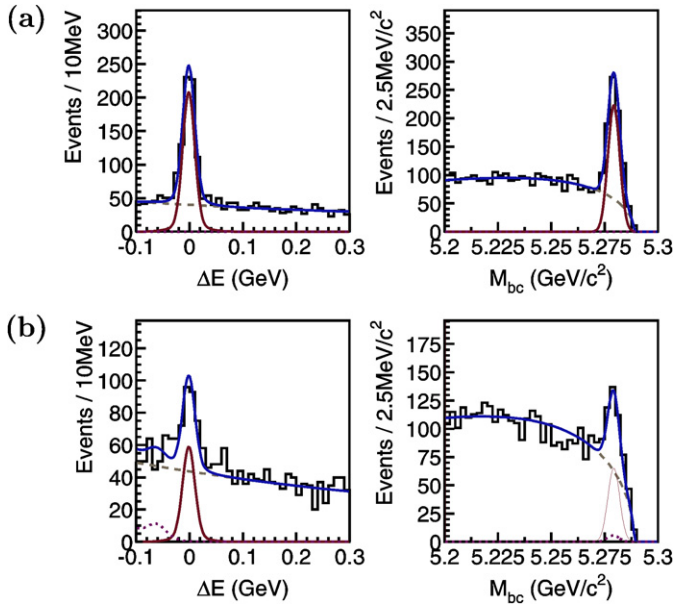

Fig. 2. Distributions of ΔE (with $M_{\rm bc} > 5.27$ GeV/c^2) and $M_{\rm bc}$ (with $|\Delta E| < 0.05$ GeV), respectively, for (a) $p\bar{p}K^+$ and (b) $p\bar{p}\pi^+$ modes with proton–antiproton pair mass less than 2.85 GeV/c^2. The solid curves, solid peaks, and dashed curves represent the combined fit result, fitted signal and fitted background, respectively. The dot-dashed curve indicates the $p\bar{p}K^+$ cross-feed background in the fit to the $p\bar{p}\pi^+$ mode.

determined by MC simulation. We then modify these parameters to account for the discrepancies between data and MC using the $p\bar{p}K^+$ signal events ($M_{p\bar{p}} < 2.85$ GeV/c^2). With this correction, we can gain about 5% more signal yield. The continuum background PDF is taken as the product of shapes in $M_{\rm bc}$ and ΔE, which are assumed to be uncorrelated. We use the parameterization first used by the ARGUS Collaboration [23], $f(M_{\rm bc}) \propto M_{\rm bc}\sqrt{1-x^2}\exp[-\xi(1-x^2)]$, to model the $M_{\rm bc}$ background, with x given by $M_{\rm bc}/E_{\rm beam}$ and ξ as a fit parameter. The ΔE background shape is modeled by a normalized second order polynomial whose coefficients are fit parameters. Because the $p\bar{p}\pi^+$ mode can contain non-negligible cross-feed events from the $p\bar{p}K^+$ mode, we include the $p\bar{p}K^+$ MC cross-feed shape in the fit for the determination of the $p\bar{p}\pi^+$ yield. The cross-feed from $p\bar{p}\pi^+$ to $p\bar{p}K^+$ is negligible. Fig. 2 illustrates the fits of the B yields in a proton–antiproton mass region below 2.85 GeV/c^2, which we refer to as the threshold-mass-enhanced region. The fitted B yields are 632^{+29}_{-28} and 184^{+19}_{-19}, for the $p\bar{p}K^+$ and $p\bar{p}\pi^+$ modes, respectively.

Since there are two different detector configurations and the detection efficiency is dependent on $M_{p\bar{p}}$, we separate the data sample into two sets and determine the B yields in bins of $M_{p\bar{p}}$, where the signal PDF is assumed to be the same for all $M_{p\bar{p}}$ bins. We generate corresponding MC samples in order to estimate the efficiencies properly. The partial branching fractions are obtained by correcting the fitted B yields for the mass dependent efficiencies for each data set; they agree well with each other for the two data sets and these results are then combined to obtain the final results.

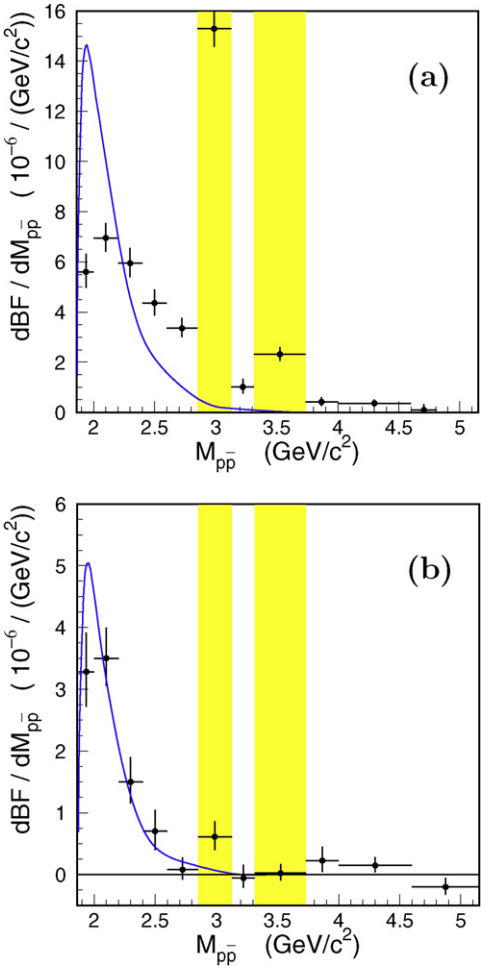

Fig. 3. Differential branching fractions for (a) $p\bar{p}K^+$ and (b) $p\bar{p}\pi^+$ modes as a function of proton–antiproton pair mass. The solid curves are theoretical predictions [11] that are scaled to the observed charmless branching fractions. The two shaded mass bins, $2.85 < M_{p\bar{p}} < 3.128$ GeV/c^2 and $3.315 < M_{p\bar{p}} < 3.735$ GeV/c^2, are not counted in the charmless signal yields since they contain contributions from the intermediate resonances η_c, J/ψ and ψ', χ_{c0}, χ_{c1} mesons, respectively.

The differential branching fractions as a function of the proton–antiproton mass for both $p\bar{p}K^+$ and $p\bar{p}\pi^+$ modes are shown in Fig. 3, and the measured branching fractions for different $M_{p\bar{p}}$ bins are listed in Tables 1 and 2. Note that we have defined the charm veto: the regions 2.850 GeV/$c^2 < M_{p\bar{p}} < 3.128$ GeV/c^2 and 3.315 GeV/$c^2 < M_{p\bar{p}} < 3.735$ GeV/c^2 are excluded to remove background from B decay modes containing an η_c, J/ψ, ψ', χ_{c0}, or χ_{c1} meson. These results supersede our previous measurements [3,8] with better accuracy. The width of the $p\bar{p}\pi^+$ mode is narrower than that of the $p\bar{p}K^+$ mode and agrees better with the theoretical expectation [10]. The error bars show the statistical uncertainties only. The listed yield is the sum from the fits for two different periods; the listed efficiency is an effective one obtained by combining the two different detector configurations.

Systematic uncertainties are determined using high-statistics control data samples. For proton identification, we use a $\Lambda \to p\pi^-$ sample, while for K/π identification we use

Table 1
The B yields from $\Delta E - M_{\rm bc}$ fits for the $B^+ \to p\bar{p}K^+$ data sample, detection efficiencies and branching fractions ($\mathcal{B}$) in different $M_{p\bar{p}}$ regions

$M_{p\bar{p}}$ (GeV/c^2)	Yield	eff (%)	$\mathcal{B}$ (10^{-6})
1.876–2.0	$95.8^{+12.0}_{-11.0}$	30.6	$0.70^{+0.09}_{-0.08}\pm0.05$
2.0–2.2	$188.0^{+16.1}_{-15.2}$	30.0	$1.39^{+0.12}_{-0.11}\pm0.09$
2.2–2.4	$146.1^{+14.1}_{-13.1}$	27.3	$1.19^{+0.12}_{-0.11}\pm0.08$
2.4–2.6	$99.9^{+12.2}_{-11.2}$	25.5	$0.87^{+0.11}_{-0.10}\pm0.06$
2.6–2.85	$100.7^{+12.0}_{-11.0}$	26.6	$0.84^{+0.10}_{-0.09}\pm0.05$
2.85–3.128	$496.8^{+23.9}_{-22.9}$	26.0	$4.25^{+0.20}_{-0.20}\pm0.28$
3.128–3.315	$20.9^{+6.8}_{-5.7}$	25.2	$0.19^{+0.06}_{-0.05}\pm0.01$
3.315–3.735	$108.2^{+13.1}_{-12.0}$	24.8	$0.97^{+0.12}_{-0.11}\pm0.06$
3.735–4.0	$11.7^{+5.9}_{-4.9}$	24.3	$0.11^{+0.05}_{-0.04}\pm0.01$
4.0–4.6	$21.9^{+9.1}_{-7.9}$	21.8	$0.22^{+0.09}_{-0.08}\pm0.01$
4.6–4.8	$1.6^{+3.2}_{-2.1}$	15.3	$0.02^{+0.05}_{-0.03}\pm0.00$
All			$10.76^{+0.36}_{-0.33}\pm0.70$
With charm veto			$5.54^{+0.27}_{-0.25}\pm0.36$
< 2.85			$5.00^{+0.24}_{-0.22}\pm0.32$

Table 2
The B yields from $\Delta E - M_{\rm bc}$ fits for the $B^+ \to p\bar{p}\pi^+$ data sample, detection efficiencies and branching fractions ($\mathcal{B}$) in different $M_{p\bar{p}}$ regions

$M_{p\bar{p}}$ (GeV/c^2)	Yield	eff (%)	$\mathcal{B}$ (10^{-6})
1.876–2.0	$51.3^{+9.5}_{-8.5}$	27.6	$0.41^{+0.08}_{-0.07}\pm0.03$
2.0–2.2	$83.1^{+12.2}_{-11.2}$	26.6	$0.70^{+0.10}_{-0.09}\pm0.05$
2.2–2.4	$32.7^{+8.9}_{-7.8}$	24.5	$0.30^{+0.08}_{-0.07}\pm0.02$
2.4–2.6	$14.8^{+7.1}_{-5.9}$	22.9	$0.14^{+0.07}_{-0.06}\pm0.01$
2.6–2.85	$1.6^{+5.5}_{-4.3}$	23.2	$0.02^{+0.05}_{-0.04}\pm0.00$
2.85–3.128	$17.5^{+7.2}_{-6.1}$	22.5	$0.17^{+0.07}_{-0.06}\pm0.01$
3.128–3.315	$-0.5^{+4.3}_{-3.0}$	22.3	$-0.01^{+0.04}_{-0.03}\pm0.00$
3.315–3.735	$0.6^{+5.6}_{-4.4}$	21.3	$0.01^{+0.06}_{-0.05}\pm0.00$
3.735–4.0	$5.5^{+5.6}_{-4.3}$	20.6	$0.06^{+0.06}_{-0.05}\pm0.00$
4.0–4.6	$8.2^{+7.9}_{-6.7}$	20.8	$0.09^{+0.08}_{-0.07}\pm0.01$
4.6–5.15	$-7.6^{+6.0}_{-4.7}$	15.8	$-0.11^{+0.08}_{-0.07}\pm0.01$
All			$1.78^{+0.23}_{-0.19}\pm0.13$
With charm veto			$1.60^{+0.22}_{-0.19}\pm0.12$
< 2.85			$1.57^{+0.17}_{-0.15}\pm0.12$

a $D^{*+} \to D^0\pi^+$, $D^0 \to K^-\pi^+$ sample. The average efficiency difference for hadron identification between data and MC has been corrected to obtain the final branching fraction measurements. The corrections are about 9% and 14% for the $p\bar{p}K^+$ and $p\bar{p}\pi^+$ modes, respectively. The uncertainties associated with the hadron identification corrections are estimated to be 4.2% for two protons and 1% for one kaon/pion. Tracking uncertainty is determined with fully and partially reconstructed D^* samples. It is about 1% per charged track. The $\mathcal{R}$ continuum suppression uncertainty is estimated from control samples with similar final states, $B^+ \to J/\psi K^+$ with $J/\psi \to \mu^+\mu^-$. The uncertainties for $\mathcal{R}$ selection are 2.5% and 4% for the $p\bar{p}K^+$ and $p\bar{p}\pi^+$ modes, respectively. A systematic uncertainty of 2% in the fit yield is determined by varying the parameters of the signal and background PDFs. The MC statistical uncertainty is less than 2%. The error on the number of $B\bar{B}$ pairs is 1.3%, where we assume that the branching fractions of $\Upsilon(4S)$ to neutral and charged $B\bar{B}$ pairs are equal. The systematic uncertainties for each decay channel are summarized in Table 3. We first sum the correlated errors linearly and then combine them with the uncorrelated ones in quadrature. The total systematic uncertainties are 6.5% and 7.4% for the $p\bar{p}K^+$ and $p\bar{p}\pi^+$ modes, respectively.

Table 3
Systematic uncertainties (%) in the branching fraction for each decay channel

Source	$p\bar{p}K^+$	$p\bar{p}\pi^+$
Tracking	3.1	3.2
Proton identification	4.2	4.2
K/π identification	1.0	1.0
Likelihood ratio selection	2.5	4.0
MC statistical error	1.4	1.8
Fitting	2.0	2.0
Number of $B\bar{B}$ pairs	1.3	1.3
Total	6.5	7.4

We study the baryon angular distribution in the proton–antiproton helicity frame at $M_{p\bar{p}} < 2.85$ GeV/c^2. The angle θ_p is defined as the angle between the baryon direction and the oppositely charged meson direction in the proton–antiproton pair rest frame, i.e. this angle is determined by p and K^-/π^-, or by $\bar{p}$ and K^+/π^+. We use the same likelihood method to estimate the B yield in each θ_p bin. Again, the signal PDF is fixed and the background shape is allowed to vary. The $\cos\theta_p$ distributions, shown in Fig. 4, for the $p\bar{p}K^+$ and $p\bar{p}\pi^+$ modes have opposite trends. This distribution for the $p\bar{p}\pi^+$ mode does not match the theoretical prediction [11], which is based on an extrapolation of the $p\bar{p}K^+$ data using the perturbative QCD framework. However, it does agree with the naive short distance picture for a $b \to u$ weak decay. Particles directly associated with b decay are more energetic and the particle containing the spectator quark is generally less energetic. After boosting to the proton–antiproton rest frame, the fast moving antiprotons and π^+'s are back-to-back most of the time. However, the $b \to s$ gluon process for the $p\bar{p}K^+$ case seems to completely disagree with this short distance picture. The baryon with the spectator quark moves faster in the B rest frame. The same phenomenon has been observed in $B^0 \to p\bar{\Lambda}\pi^-$ [24] decays. Another theoretical prediction proposes a long distance effect, namely $p\bar{p}$ rescattering through a hypothetical baryonium bound state [12], in order to explain the violation of the short distance picture for the $p\bar{p}K^+$ mode. Since this long distance effect should also occur for the $p\bar{p}\pi^+$ case, it seems that further theoretical investigations are needed to simultaneously explain the behavior of both the $p\bar{p}K^+$ and $p\bar{p}\pi^+$ modes.

Because we have enough $B^+ \to p\bar{p}K^+$ signal events in the threshold enhancement region, we separate this region into five sub-regions. Fig. 5(a)–(e) shows the efficiency corrected B

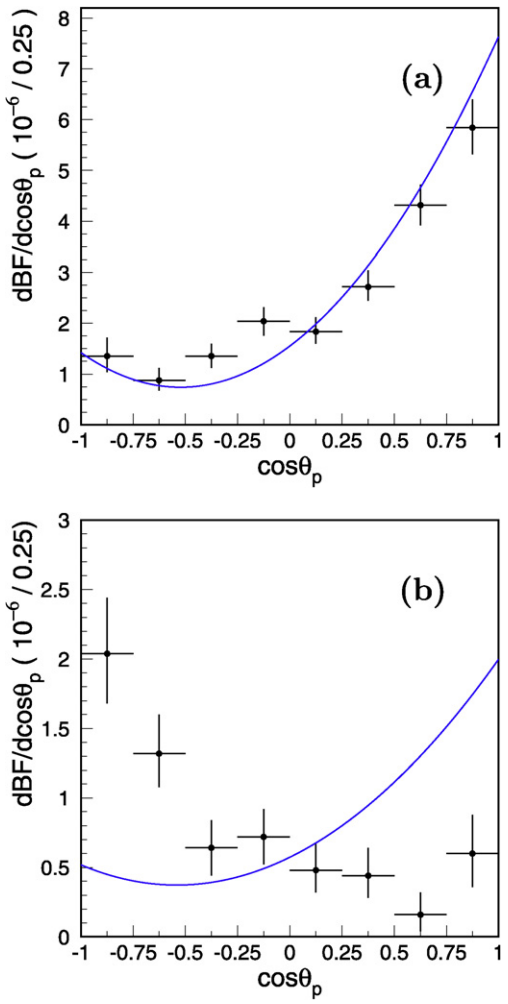

Fig. 4. Differential branching fractions *vs.* $\cos\theta_p$ in the proton–antiproton pair system for (a) $B^+ \to p\bar{p}K^+$ and (b) $B^+ \to p\bar{p}\pi^+$. The solid curve is the theoretical prediction [11].

yield as a function of $\cos\theta_p$ for these five sub-regions. We define the angular asymmetry as $A_{\theta_p} = \frac{N_+ - N_-}{N_+ + N_-}$, where N_+ and N_- stand for the efficiency corrected B yield with $\cos\theta_p > 0$ and $\cos\theta_p < 0$, respectively. The measured angular asymmetry as a function of $M_{p\bar{p}}$ is shown in Fig. 5(f). It is interesting to see that there is a clear trend, which indicates that the relative contributions from two (or more) competing decay amplitudes are changing in this mass range. The measured average A_{θ_p} value of the threshold enhancement is given in Table 4. The systematic error, ~ 0.03, is determined by checking the $B^+ \to J/\psi K^+$ ($J/\psi \to \mu^+\mu^-$) sample and the continuum background in $B^+ \to p\bar{p}K^+$ where no asymmetry is expected. The observed A_{θ_p}'s are 0.02 ± 0.01 for $B^+ \to J/\psi K^+$ and 0.00 ± 0.02 for the continuum background.

We also search for the intermediate two-body decays, $B^+ \to \bar{p}\Delta^{++}$ ($\Delta^{++} \to p\pi^+$) and $B^+ \to p\bar{\Delta}^0$ ($\bar{\Delta}^0 \to \bar{p}\pi^+$), from the $p\bar{p}\pi^+$ three-body final state. Events with $M_{p\pi} < 1.4$ GeV/c^2 are selected. No significant signals are found from the likelihood fit in those decay chains. We observe 59 and 86 events in the signal box; the expected numbers of background events from the fits are 73.0 ± 1.6 and 81.4 ± 1.6 for $B^+ \to \bar{p}\Delta^{++}$ and $B^+ \to p\bar{\Delta}^0$, respectively. We set upper limits on the branching fractions at the 90% confidence level using the methods described in Refs. [25,26] where the 7.4% systematic uncertainty for $B^+ \to p\bar{p}\pi^+$ is taken into account. The results are $\mathcal{B}(B^+ \to \bar{p}\Delta^{++}) < 0.14 \times 10^{-6}$ and $\mathcal{B}(B^+ \to p\bar{\Delta}^0) < 1.38 \times 10^{-6}$. These numbers are smaller than the theoretical expectations but agree with other experimental findings [27].

Since there is a prediction [28] that direct CP violation in $B^+ \to J/\psi K^+$ is at the 1% level, it is quite possible that this effect could be magnified due to the interference [29] between the resonance and the threshold enhancement. We define the charge asymmetry $A_{\rm CP}$ as $(N_b - N_{\bar{b}})/(N_b + N_{\bar{b}})$ for the $p\bar{p}K^+$ and $p\bar{p}\pi^+$ modes, where N_b ($N_{\bar{b}}$) stands for the efficiency corrected B^- (B^+) yield. The selection criteria for J/ψ (η_c) and

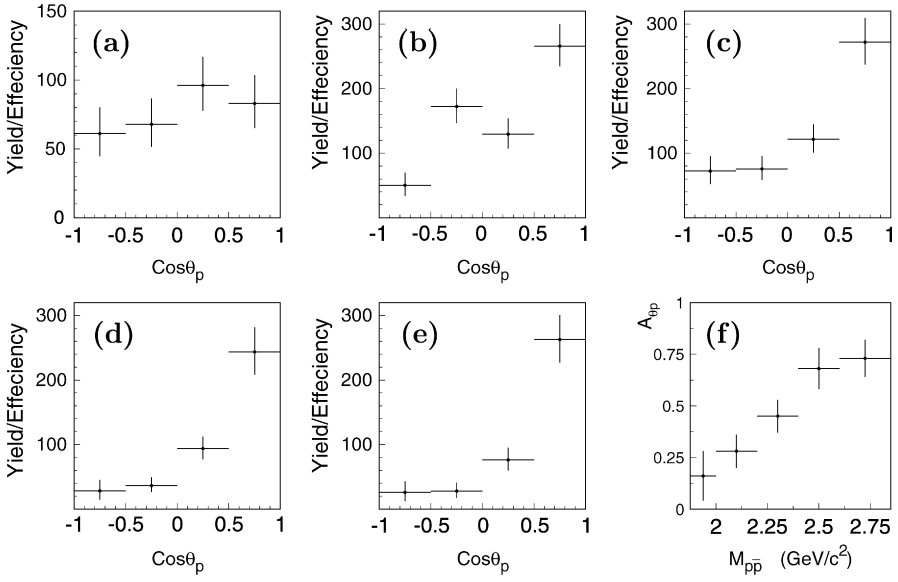

Fig. 5. Efficiency corrected B yield *vs.* $\cos\theta_p$ for (a) $M_{p\bar{p}} < 2.0$ GeV/c^2, (b) $2.0 < M_{p\bar{p}} < 2.2$ GeV/c^2, (c) $2.2 < M_{p\bar{p}} < 2.4$ GeV/c^2, (d) $2.4 < M_{p\bar{p}} < 2.6$ GeV/c^2, and (e) $2.6 < M_{p\bar{p}} < 2.85$ GeV/c^2; (f) the measured angular asymmetries (A_{θ_p}) for these five mass regions near threshold.

Table 4
Summary of the results in the mass region $M_{p\bar{p}} < 2.85$ GeV/c^2 and in other intermediate resonance regions. Y is the fitted signal yield (or upper limit at 90% confidence level), $\mathcal{B}$ is the branching fraction, A_θ is the angular asymmetry and A_{CP} is the charge asymmetry

Mode	Y	$\mathcal{B}$ (10^{-6})	A_θ	A_{CP}
$p\bar{p}K^+$	632^{+29}_{-28}	$5.00^{+0.24}_{-0.22} \pm 0.32$	$0.45 \pm 0.05 \pm 0.03$	$-0.02 \pm 0.05 \pm 0.02$
$\eta_c K^+$	158^{+14}_{-13}	–	–	$-0.16 \pm 0.08 \pm 0.02$
$J/\psi K^+$	236^{+16}_{-16}	–	–	$0.09 \pm 0.07 \pm 0.02$
$p\bar{p}\pi^+$	184^{+19}_{-19}	$1.57^{+0.17}_{-0.15} \pm 0.12$	$-0.47 \pm 0.12 \pm 0.03$	$-0.17 \pm 0.10 \pm 0.02$
$\bar{p}\Delta^{++}$	< 7.5	< 0.14	–	–
$p\bar{\Delta}^0$	< 25.9	< 1.38	–	–

related consistency checks have been reported in Ref. [30]. We adopt the same criteria and assume the signal PDFs are the same for both B^- and B^+ samples. The results from the likelihood fits are listed in Table 4 for various mass/resonance regions. No significant charge asymmetries are found. The systematic uncertainty is assigned using the measured charge asymmetry for sideband data and is found to be -0.01 ± 0.01.

In summary, using $449 \times 10^6 B\bar{B}$ events, we measure the mass and the angular distributions of the proton–antiproton pair system near threshold for the $p\bar{p}K^+$ and $p\bar{p}\pi^+$ baryonic B decay modes. These results supersede our previous measurements [3,8] with better accuracy. The width of the threshold enhancement in the $p\bar{p}\pi^+$ mode is narrower than that of the $p\bar{p}K^+$ mode and agrees better with the theoretical expectation [10]. The proton polar angular distributions of the $p\bar{p}K^+$ and $p\bar{p}\pi^+$ modes have opposite trends. This shows that the $b \to s$ and $b \to u$ processes are kinematically different at short distance. We also search for intermediate two-body decays in the $p\bar{p}\pi^+$ final states; no significant signals are found.

Acknowledgements

We thank the KEKB group for the excellent operation of the accelerator, the KEK cryogenics group for the efficient operation of the solenoid, and the KEK computer group and the National Institute of Informatics for valuable computing and Super-SINET network support. We acknowledge support from the Ministry of Education, Culture, Sports, Science, and Technology of Japan and the Japan Society for the Promotion of Science; the Australian Research Council and the Australian Department of Education, Science and Training; the National Science Foundation of China and the Knowledge Innovation Program of the Chinese Academy of Sciences under contract No. 10575109 and IHEP-U-503; the Department of Science and Technology of India; the BK21 program of the Ministry of Education of Korea, the CHEP SRC program and Basic Research program (grant No. R01-2005-000-10089-0) of the Korea Science and Engineering Foundation, and the Pure Basic Research Group program of the Korea Research Foundation; the Polish State Committee for Scientific Research; the Ministry of Education and Science of the Russian Federation and the Russian Federal Agency for Atomic Energy; the Slovenian Research Agency; the Swiss National Science Foundation; the National Science Council and the Ministry of Education of Taiwan; and the US Department of Energy.

References

[1] K. Abe, et al., Belle Collaboration, Phys. Rev. Lett. 88 (2002) 181803.
[2] M.Z. Wang, et al., Belle Collaboration, Phys. Rev. Lett. 90 (2003) 201802.
[3] M.Z. Wang, et al., Belle Collaboration, Phys. Rev. Lett. 92 (2004) 131801.
[4] Y.J. Lee, et al., Belle Collaboration, Phys. Rev. Lett. 93 (2004) 211801.
[5] Y.J. Lee, et al., Belle Collaboration, Phys. Rev. Lett. 95 (2005) 061802.
[6] W.S. Hou, A. Soni, Phys. Rev. Lett. 86 (2001) 4247.
[7] C.K. Chua, W.S. Hou, S.Y. Tsai, Phys. Lett. B 544 (2002) 139;
J.L. Rosner, Phys. Rev. D 68 (2003) 014004;
B. Kerbikov, A. Stavinsky, V. Fedotov, Phys. Rev. C 69 (2004) 055205;
J. Haidenbauer, U.-G. Meissner, A. Sibirtsev, Phys. Rev. D 74 (2006) 017501;
D.R. Entem, F. Fernandez, Phys. Rev. D 75 (2007) 014004.
[8] M.Z. Wang, et al., Belle Collaboration, Phys. Lett. B 617 (2005) 141;
B. Aubert, et al., BaBar Collaboration, Phys. Rev. D 72 (2005) 051101.
[9] H.Y. Cheng, Int. J. Mod. Phys. A 21 (2006) 4209.
[10] C.K. Chua, W.S. Hou, S.Y. Tsai, Phys. Rev. D 66 (2002) 054004.
[11] C.Q. Geng, Y.K. Hsiao, Phys. Rev. D 74 (2006) 094023.
[12] M. Suzuki, J. Phys. G 34 (2007) 283.
[13] N. Gabyshev, et al., Belle Collaboration, Phys. Rev. Lett. 90 (2003) 121802;
N. Gabyshev, et al., Belle Collaboration, Phys. Rev. Lett. 97 (2006) 242001;
R. Chistov, et al., Belle Collaboration, Phys. Rev. D 74 (2006) 111105(R).
[14] V.L. Chernyak, I.R. Zhitnitsky, Nucl. Phys. B 345 (1990) 137.
[15] M. Jarfi, et al., Phys. Rev. D 43 (1991) 1599;
H.Y. Cheng, K.C. Yang, Phys. Rev. D 66 (2002) 014020.
[16] C.K. Chua, Phys. Rev. D 68 (2003) 074001.
[17] S. Kurokawa, E. Kikutani, Nucl. Instrum. Methods A 499 (2003) 1, and other papers included in this volume.
[18] A. Abashian, et al., Belle Collaboration, Nucl. Instrum. Methods A 479 (2002) 117.
[19] Z. Natkaniec, Belle SVD2 Group, Nucl. Instum. Methods A 560 (2006) 1.
[20] R. Brun, et al., GEANT 3.21, CERN Report No. DD/EE/84-1, 1987.
[21] R.A. Fisher, Ann. Eugenics 7 (1936) 179.
[22] K. Abe, et al., Belle Collaboration, Phys. Lett. B 517 (2001) 309.
[23] H. Albrecht, et al., ARGUS Collaboration, Phys. Lett. B 241 (1990) 278;
H. Albrecht, et al., ARGUS Collaboration, Phys. Lett. B 254 (1991) 288.
[24] M.Z. Wang, et al., Belle Collaboration, arXiv: 0704.2672.
[25] G.J. Feldman, R.D. Cousins, Phys. Rev. D 57 (1998) 3873.
[26] J. Conrad, et al., Phys. Rev. D 67 (2003) 012002.
[27] Y.-T. Tsai, et al., Belle Collaboration, Phys. Rev. D 75 (2007) 111101.
[28] W.S. Hou, M. Nagashima, A. Soddu, hep-ph/0605080.
[29] M. Hazumi, Phys. Lett. B 583 (2004) 285.
[30] C.-H. Wu, et al., Belle Collaboration, Phys. Rev. Lett. 97 (2006) 162003.